Astronomy & Astrophysics

Multiple and changing cycles of active stars

II. Results

K. Oláh[1], Z. Kolláth[1], T. Granzer[2], K. G. Strassmeier[2], A. F. Lanza[5], S. Järvinen[2,6,7], H. Korhonen[3], S. L. Baliunas[4], W. Soon[4], S. Messina[5], and G. Cutispoto[5]

[1] Konkoly Observatory of the Hungarian Academy of Sciences, 1525 Budapest, Hungary
   e-mail: olah@konkoly.hu
[2] Astrophysical Institute Potsdam (AIP), An der Sternwarte 16, 14482 Potsdam, Germany
[3] ESO, Karl-Schwarzschild Strasse 2, 85748 Garching bei Munchen, Germany
[4] Harvard - Smithsonian Center for Astrophysics, Cambridge, MA 02138, USA
[5] INAF - Osservatorio Astrofisico di Catania, via S. Sofia 78, 95123 Catania, Italy
[6] Tuorla Observatory, University of Turku, 21500 Piikkiö, Finland
[7] Astronomy Division, PO Box 3000, 90014 University of Oulu, Finland

ABSTRACT

Aims. We study the time variations in the cycles of 20 active stars based on decade-long photometric or spectroscopic observations.
Methods. A method of time-frequency analysis, as discussed in a companion paper, is applied to the data.
Results. Fifteen stars definitely show multiple cycles, but the records of the rest are too short to verify a timescale for a second cycle. The cycles typically show systematic changes. For three stars, we found two cycles in each of them that are not harmonics and vary in parallel, indicating a common physical mechanism arising from a dynamo construct. The positive relation between the rotational and cycle periods is confirmed for the inhomogeneous set of active stars.
Conclusions. Stellar activity cycles are generally multiple and variable.

Key words. stars: activity – stars: atmospheres – stars: late-type – starspots

1. Introduction

In the middle of the last century it was realised that certain observed features of late-type stars could be explained by magnetic phenomena (Kron 1947), similar to those detected on the Sun. The cyclic pattern of solar activity had already been known for more than 120 years (Schwabe 1843) by the time systematic research of the magnetic activity of late-type stars commenced. In 1966 long-term monitoring of the relative fluxes of cores of the CaII lines – thought to indicate the strength and coverage of surface magnetism through the enhancement of chromospheric flux in the line cores – of solar type stars began (cf. Wilson 1968) to search for stellar cycles analogous to the solar case, and that monitoring program continued for more than three decades. Eleven years after systematic monitoring had begun, Wilson (1978) published landmark results from the first decadal survey of chromospheric variability and stellar magnetic cycles.

While Wilson was early in his observational work, a contemporary comment on the possibility of the existence of stellar cycles appeared in an editorial note by Detre (1971) to a paper presenting photometric observations of BY Dra by P. F. Chugainov, as follows: *The continuous observation of Chugainov's stars would be extremely important because diagrams like that on the opposite page may reveal the existence of cycles similar to the solar cycle in these stars.*

Studying the late type eclipsing binary XY UMa, Geyer (1978) suggested an activity cycle to explain the outside-eclipse variability of the system. Durney & Stenflo (1972) presented a first theoretical forecast, namely with increasing rotation rate,

cycle periods should be decreasing. Baliunas et al. (1996b) summarised knowledge on the dynamo interpretation of stellar activity cycles prior to 1996.

As databases relevant to decadal stellar activity continued to lengthen and contain more stars, study began of the variability of stellar activity cycles. Multiple cycles, analogous to the known solar multicyclic variability, were recovered by Baliunas et al. (1996b) from the records of the Ca II index. Using these Ca index data supplemented with photometric results of active dwarfs and giants, Saar & Brandenburg (1999) studied the time variability of stellar cycles and multiple cycles on the evolutionaly timescale, drew the distribution of P_{rot}/P_{cyc} in the function of the Rossby number, and compared the results with theoretical models.

At the beginning of the current century, several photometric records became long enough to study photospheric magnetic cycles on a relatively large sample of active stars. Using conventional methods, Oláh et al. (2000, 2002) derived activity cycles and multicycles for most objects in the present investigation, and Messina & Guinan (2002) for six young solar analogues. Radick et al. (1998) investigated the relation between the Ca index and contemporaneous photometric measurements on 35 Sun-like stars. Lockwood et al. (2007) studied the magnetic cycle patterns seen in the photospheres and chromospheres of 32 stars primarily on or near the lower main sequence. In both those last two papers, it was found that, on a decadal scale, younger stars decrease in brightness when their chromosperic activity increases, while the older, less active stars increase in brightness when chromospheric activity increases, as is the case

for the Sun. The existence and relation of photospheric and chromospheric cycles are well established.

On the basis of the variability of the 11-yr solar cycle, which fluctuates between approximately 9 and 14 years, and the assumption that stellar activity shares properties similar to solar activity, one may presume that stellar cycles should also show multidecadal variability. The first attempt to follow *changing stellar activity cycles* was made by Frick et al. (1997), who developed and applied a modified wavelet technique suitable for data with gaps and found a variable cycle of one of the targets in the present investigation, HD 100180, from its Ca II index record. Subsequent work by Frick et al. (2004) and Baliunas et al. (2006) used double-wavelet analysis of the records of stars in the Wilson sample to study interdecadal activity variations.

Recent efforts have focused on methods of *predicting* solar activity based on different, earlier observations and on dynamo theory. For critical reviews of those methods see Cameron & Schüssler (2007), and Bushby & Tobias (2007). The knowledge of the cycle pattern of as many active stars as possible may yield improved insight on the solar activity seen in the context of stellar activity. To that end, we have developed a method suited to studying multi-decadal variability from gapped datasets. The method is presented in detail by Kolláth & Oláh (2009, hereafter Paper I), where it is applied to solar data and used to recover a complicated pattern of multi-scale variability of the Sun in the past few hundred years. In the current paper we apply the method to a sample of active stars with photometric or spectroscopic records that extend over several decades.

2. Observations

2.1. The sample

The most important criterion for the selection of stars for analysis was a long record with few interruptions. In most of the cases gaps in the records are seasonal interruptions, and we require that the gap does not exceed two seasons. Limited gaps are crucial because the method of analysis requires equidistant data, and therefore interpolation during gaps in the data (i.e., between observing seasons) is necessary.

The stellar sample consists of 21 objects, with the Sun studied in Paper I. Most of the stars have photometric records, V833 Tau has a century-long record if augmented by photographic photometry, and six stars have Ca II index records. The photometrically observed active stars are listed in Table 1 together with their rotational (or orbital) periods, spectral types, $v \sin i$, and inclination. The last column lists the extent of the records in years. Single stars are AB Dor, LQ Hya, V410 Tau, and FK Com (about its possible binarity see Kjurkchieva & Marchev 2005), and the rest (V833 Tau, EI Eri, V711 Tau, UZ Lib, UX Ari, HU Vir, IL Hya, XX Tri, HK Lac, and IM Peg) are synchronised, close binaries. In the case of binaries Table 1 gives the orbital period and the rotational period for single stars. In addition we study six objects from the Wilson sample (Wilson, 1978): HD 131156A, HD 131156B, HD 100180, HD 201091, HD 201092, and HD 95735. In our analysis, those targets are considered to be single or effectively single stars, since HD 131156A with HD 131156B and HD 201091 with HD 201092 form wide, visual binaries. Their rotational periods, spectral types, and length of the Ca index records are listed in Table 2.

Table 1. The stellar sample. I. Photometric observations.

Star	Rot. Per.[a] (days)	Sp. type	$v \sin i$ (km s^{-1})	i (°)	Time-base (years)
AB Dor	0.515	K0V	91	60	18
LQ Hya	1.601	K2V	27	65	25
V833 Tau	1.788	K5V	6.3	20	20
"	photographic + photometric data				109
V410 Tau	1.872	K4	74	70	34
EI Eri	1.947	G5IV	51	46	28
FK Com	2.400	G4III	155	60	28
V711 Tau	2.838	G5IV/K1IV	41	40	30
UZ Lib	4.768	K0III	67	50	17
UX Ari	6.437	G5V/K0IV	39	60	23
HU Vir	10.388	K1IV-III	25	65	17
IL Hya	12.905	K0III-IV	26.5	55	20
XX Tri	23.969	K0III	21	60	21
HK Lac	24.428	K0III	20	65	50
IM Peg	24.649	K2III-II	26.5	70	29

The stellar parameters are from Strassmeier (2002), and the references therein. [a] The orbital period is given in case of synchronised binary.

Table 2. The stellar sample. II. Ca index measurements.

Star	Rot. per. (days)	Sp. type	Time-base (years)
HD 131156A = ξ Boo A	6.25	G8V	35
HD 131156B = ξ Boo B	11.1	K4Ve	35
HD 100180 = 88 Leo	14.3	G0V	34
HD 201092 = 61 Cyg B	35.5	K7V	35
HD 201091 = 61 Cyg A	36.1	K5V	35
HD 95735 = GJ 411	54.7	M2V	34

2.2. Multi-decadal photometry

The photometric records contain all the published material for each star in the sample, in *V*-colour. Those stars are well-studied, with numerous papers describing the records. Recent summaries for the stars are as follows: AB Dor: Järvinen et al. (2005); LQ Hya: Berdyugina et al. (2002) and Kővári et al. (2004); V833 Tau: Oláh et al. (2001); V410 Tau: Strassmeier et al. (1997b); EI Eri: Strassmeier et al. (1997b); FK Com: Oláh et al. (2006); V711 Tau: Lanza et al. (2006) and Strassmeier et al. (1997b); UZ Lib: Oláh et al. (2002); UX Ari: Aarum-Ulvås & Henry (2003); HU Vir: Strassmeier et al. (1997b); IL Hya: Strassmeier et al. (1997b); XX Tri: Strassmeier et al. (1997b); HK Lac: Oláh et al. (1997); IM Peg: Ribárik et al. (2003). The records for several stars were updated through 2007–2008 using new photometry from the Vienna APT (Strassmeier et al. 1997a).

For more details, see the references of the cited papers. Periods of sparsely-sampled data leading to large gaps, sometimes seen in the onset of records, were disregarded.

2.3. Ca II index measurements

The Ca II measurements were collected at the Mount Wilson Observatory, with two sets of equipment on two different telescopes, from 1966 to 1978 and after, for details see Vaughan et al. (1978). The relative Ca emission is the flux ratio of two 0.1 nm passbands centred on the cores of the H and K lines and two 2 nm passbands in the nearby continuum.

3. Method

We applied a time-frequency analysis called short-term Fourier transform (STFT) to the photometric and spectroscopic records
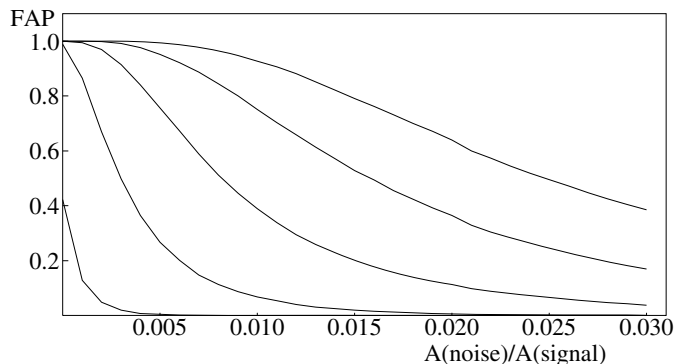
Fig. 1. False alarm probability that a structure appears in STFT when Gaussian noise, with different amplitudes, is added to the record of LQ Hya. Five different standard deviations were used and the results are plotted from left to right for σ_n = 0.01, 0.02, 0.03, 0.04, 0.05 mag. Details are in the text.

to study the time variability of the activity cycles that occur in the sample of twenty stars. As stated earlier, the analysis requires equidistant data, so that we had to interpolate through gaps among observations. To interpolate, we used a smoothing spline. Before calculating the spline interpolation, we removed the rotational signal and the next four strongest components in the periodogram near the rotation period; the removal of the next four strongest signals addresses removal rotation signals that are non-sinusoidal in shape or other activity changes on similar time scales from the record. Because rotational modulation is subject to change owing to differential rotation, removing the rotational signal (and the additional signals of similar timescale) was done separately for subsets in the record, typically around 200 days long, which were then averaged for the spline interpolation. We argue that such a procedure is necessary, because unevenly sampled rotational modulation may alter the average seasonal light level, and consequently cause a false signal in the analysis for multidecadal variability. This step is especially important for stars with high amplitude rotational modulation, arising from, e.g., high axial inclination to our line of sight. The FWHM of the Gaussian used in the time series is usually ~180 days. In the actual calculation however, we use filtering in the Fourier space instead of temporal filtering. The method is explained in detail in Paper I, where tests of the effects of seasonal gaps, rotational modulation, and observational errors are also found.

The effect of active region growth and decay, as discussed by Messina & Guinan (2003) has little influence on our results because we removed the rotational frequencies plus four other signals on a similar timescale, thereby significantly reducing the amplitudes of the modulation due to rotation, in most cases. Moreover, cycles below about 1.5–2 years are not considered significant, as was discussed in Paper I and below.

To check the effect of added Gaussian noise on false features in the time-frequency diagram, we performed a Monte-Carlo simulation. Here we present the results of that test on the record of LQ Hya as an example; data of other stars in the sample are of similar quality. First, Gaussian noise was added to the original observational record. We performed the same pre-processing (averaging and spline-smoothing interpolation) as for the standard processing of the actual records. The STFT of the difference between the noisy and the original smoothed data was calculated, and the statistics of the maximum amplitude (largest peak or ridge) was estimated from 10 000 cases. Figure 1 shows the false alarm probability $FAP(z)$, e.g. the probability that a

structure with amplitude larger than $z = A(\text{noise})/A(\text{obs})$ appears in STFT owing to noise ($A(\text{noise})$), and $A(\text{obs})$ is the maximum amplitude in STFT; i.e., z is the inverse of the signal-to-noise ratio). The test was performed with different standard deviations (σ_n) of the added Gaussian noise. On the figure from left to right the curves belonging to σ_n = 0.01, 0.02, 0.03, 0.04, 0.05 mag are displayed. In the case of Gaussian noise ~0.01–0.02 mag – which is poorer precision than typical photometric precision – the probability of false signals with amplitudes over 0.01th of the highest signal is less than 10% and decreases fast toward larger astrophysical amplitudes.

4. Results of the time-series analysis from photometric data

From analysis of the records we found changing and multiple cycles for most of the stars. Below we present a short description of the cycle pattern for each object. The records and STFT results are plotted in Fig. 2.

In the time-frequency plots darker colours mean higher amplitudes. The signals are modified by different amplification factors that are employed to make the smaller amplitude signals more visible (see Paper I for more). The amplification factors are given in Table 3. It is not straightforward to estimate the significance of the signals; moreover, no independent measure can be given. We consider a cycle or cycles to be significant if at least two of these three features are true: a) the signal runs throughout the period of the observations; b) it has high amplitude; or c) when two or more components are changing parallel. Cycles shorter than about 1.5–2 years are considered to be insignificant: we showed in Paper I that, from datasets having yearly gaps such cycles cannot be recovered safely. On the other hand, a long-term cycle is not significant if its length is commensurable to the time span of the observations, i.e., when the data do not cover approximately two full cycles.

AB Dor. The record of AB Dor is not well-sampled, the number of observations per year is low, and gaps longer than two years occur twice. The only clear signal is a cycle ~3.3-yr. The other, weaker signal of ~2-yr appears in the beginning of the record and is not considered reliable, possibly owing to under-sampling. Variability of high amplitude is reported on the time scale of ~20-yr (Innis et al. 2008), but the record is not long enough to be verified from our analysis.

LQ Hya. This star is a fast-rotating, single star, one of the most interesting targets. The light variation is well-sampled by the measurements and all gaps are less than one year long. Previously, cycles between 11.4–11.6 years, 6.8–6.5 years, and 2.8–3.2 years were determined by Oláh et al. (2000, 2002) from observations spanning a shorter period, and more recently, cycles of 13.8 ± 2.8-yr, and its harmonic 6.9 ± 0.8 and 3.7 ± 0.3-yr were found from long-term photometry by Kővári et al. (2004). The present analysis recovers two short cycles ~2.5 and 3.6-yr, the latter being stronger in the middle of the dataset. Another cycle ~7-yr is present, and that period increases continuosly to 12.4 years with the same amplitude, while a small amplitude ~7-yr signal remains.

V833 Tau. The short (20-yr) photometric record of this binary was supplemented by archive photographic data (Hartmann et al. 1981), thereby extending the dataset to 109 years. We analysed separately the well-sampled short and more sparse, long records. The long one includes the photometric data. The short photometric record shows two modulations, with the weaker ~2.2-yr long and the stronger ~5.2–5.5-yr. Both are
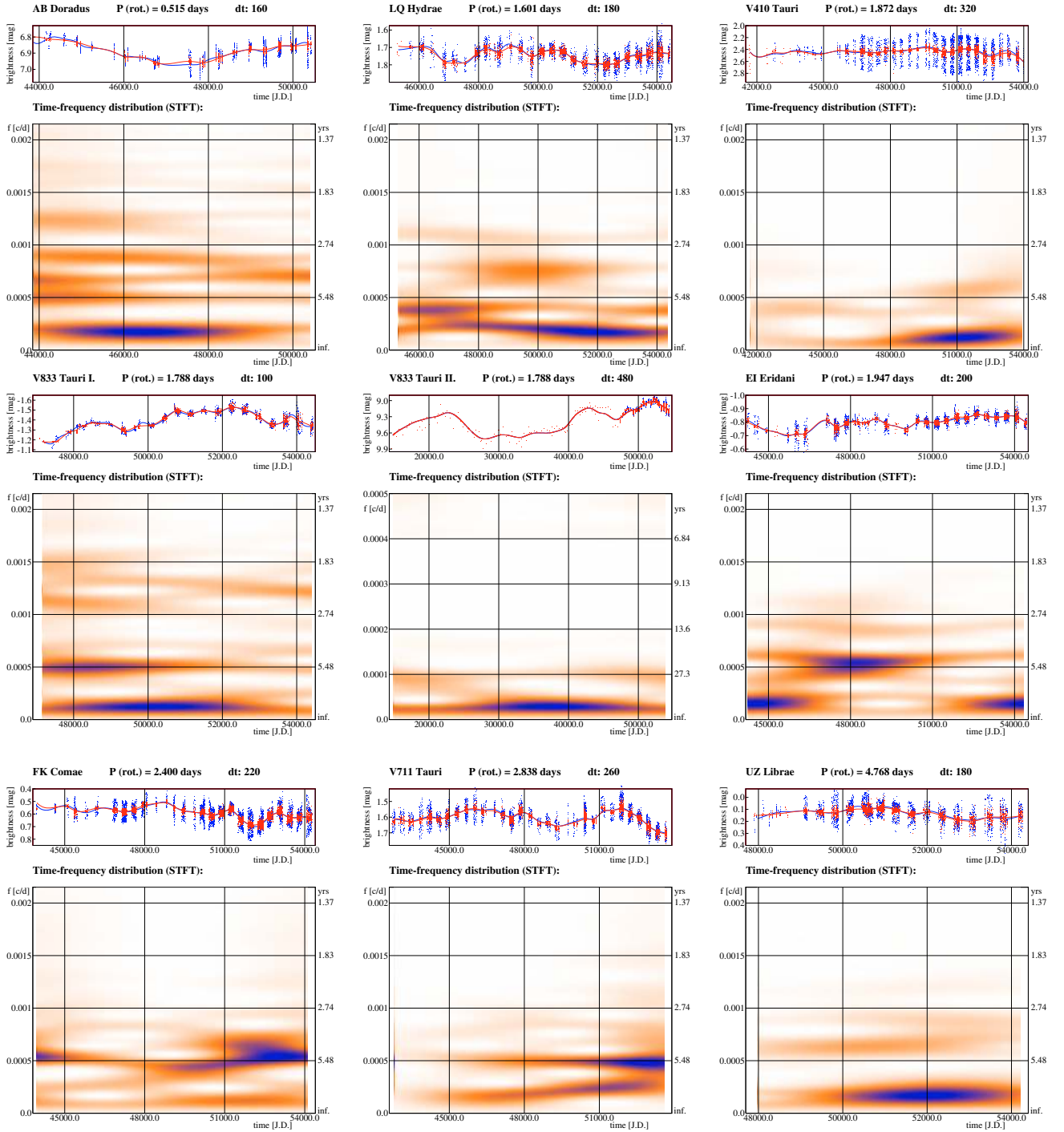
Fig. 2. Results of the STFT analysis. In the upper panel for each segment (i.e., for each star) the observational data (grey, blue in the electronic version), the data prewhitened with the mean rotational periods and the next four strongest signals for each data subset (black, red in the electronic version), and the corresponding spline interpolations (solid grey (blue) and black (red) lines) are plotted. The lengths of the data subsets are given in the top line of each segment. *The lower panels* show the time-frequency distributions, where darker colours denote higher amplitudes. The amplitudes are also modified by the amplification factors (see Table 3). *Top*: AB Dor, LQ Hya, V410 Tau. *Middle*: V833 Tau photometric data, V833 Tau photographic+photometric data, EI Eri. *Bottom*: FK Com, V711 Tau, UZ Lib. Details are in the text.

present throughout the record, which agrees with our previous results (Oláh et al. 2000, 2002). The rotational modulation has a small amplitude (few hundredths of magnitude) resulting from the low inclination of the star (≈20°). This low amplitude of rotation modulation is an important fact when we study the century-long dataset from the archive photographic measurements, even though only 1–2 points/year are available in Hartmann et al. (1981). However, those data represent the stellar brightness, within the usual error of the photographic measurements of ~0.1 mag, because the rotational modulation itself has a lower amplitude than this value. Thus, a cycle amplitude above ~0.1 mag is documented well by the photographic record
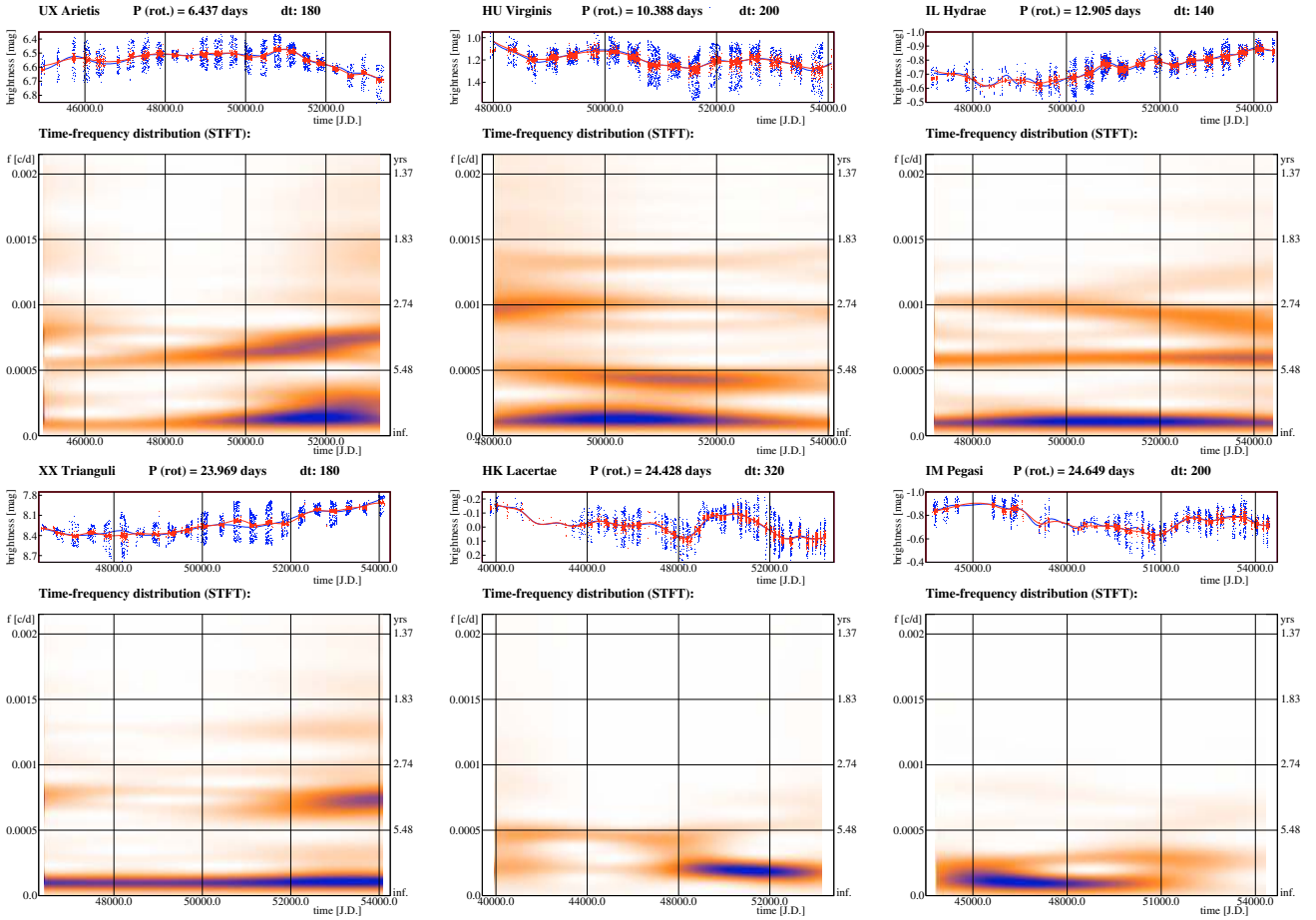
Fig. 2. continued. Results of the STFT analysis. *Top*: UX Ari, HU Vir, IL Hya. *Bottom*: XX Tri, HK Lac, IM Peg. Details are in the text.

and is considered real. A long-term modulation is present during the 109-yr period of observations, with a large amplitude of ~0.9 mag. A long cycle of ~27–30-yr is also recovered.

V410 Tau. This is the only T Tauri-type star in the sample. V410 Tau shows rotational modulation with a large amplitude (often ~0.5–0.7 mag). However, its mean brightness has remained within ~0.2 mag during the 34-yr length of the record. The analysis reveals a small-amplitude cycle of ~6.5–6.8-yr, which abruptly changes to 5.2-yr near JD 2 449 500 and afterward slowly decreases in period. The long-term trend seems to follow this decrease. Our result supports that of Stelzer et al. (2003), who found ~5.4-yr cycle in yearly mean magnitudes after 1990 (~2 448 500). While Steltzer et al. points out that the cycle had been out of phase in the earlier observations, we suggest a different, longer, and slowly variable cycle length in the beginning of the record.

EI Eri. In the recently available record covering 28 years, two short cycles of ~2.9–3.1-yr and ~4.1–4.9-yr are present. They smoothly and in parallel increase and decrease; the longer one has a high amplitude between JD 2 446 000–50 000. A long cycle of ~14-yr with variable amplitude is also seen. Two cycles of ~2.4 and ~16.2-yr has been found earlier by Oláh et al. (2000). Subsequently, using a longer record, Oláh et al. (2002) confirmed the ~2.4-yr cycle and revised the longer one to ~12.2-yr. The first determination of the long cycle was 11 ± 1 years by Strassmeier et al. (1997b), and all determinations of the long cycle point to an approximate decadal cycle. Rotational periods of EI Eri in different seasons has been

investigated in detail by Washuettl et al. (2008), and no correlation is found between the seasonal periods (or multiperiods owing to differential rotation of 2–3 active regions at different latitudes for most seasons) and the cycle pattern.

FK Com. One dominant cycle is present in the record changing smoothly between 4.5 and 6.1-yr. This is consistent with the earlier result by Oláh et al. (2006), who found quasiperiods of about 5.2 and 5.8-yr in the longitudes of starspots, based on a record of 18 years, between JD 2 446 800–53 200 (1987–2004).

V711 Tau. The 30-yr record has the best observational coverage in our sample. The observations themselves show two waves of ~18 and 9-yr, and they are clearly defined in the time-frequency diagram. Apart from those two periods, a cycle of ~5.4-yr is present throughout most of the record. A short, weak cycle of ~3.3-yr is also apparent from JD 2 445 000 onwards. Several papers give estimates of the cycles of this well-observed system, and all are in accordance with the present results: Henry et al. (1995) suggests a cycle of ~5.5 ± 0.3-yr and some evidence for a long one of ~16 ± 1-yr from photometry, Vogt et al. (1999) reported short cycles of ~3.0 ± 0.2 and ~2.7±0.2-yr for the polar spot area and for the low-latitude spots from Doppler images. Lanza et al. (2006) use a longer record of photometry to find a cycle of ~3–5-yr with variable amplitude and a longer cycle, ~19.5 ± 2.0-yr. Berdyugina & Henry (2007) use an inversion technique on photometric data between 1975–2006 to find ~5.3 ± 0.1 and 15–16-yr cycles. Taking all these independent results into account both from photometry and spectroscopy, the cycle pattern of V711 Tau is well documented.

Table 3. Amplification factors for the different frequency intervals.

Star	Frequency (1/d) interval	Ampl. factor	Frequency (1/d) interval	Ampl. factor	Frequency (1/d) interval	Ampl. factor	Start-end JD −2 400 000 d
AB Dor	0.0–0.0004	0.7	0.00041–	4.0			43 856-50 438
LQ Hya	0.0–0.0005	1.0	0.00051–	2.5			45 275-54 450
V833 Tau I.	0.0–0.0004	1.0	0.00041–0.001	2.0	0.0011–	5.0	47 098-54 450
V833 Tau II.	0.0–0.0004	0.8	0.00041–0.001	5.0	0.0011–	9.0	14 643-54 450
V410 Tau	0.0–	1.0					41 675-54 011
EI Eri	0.0–0.00035	1.0	0.00036–	3.5			44 129-54 450
FK Com	0.0–0.0002	1.0	0.00021–0.0006	2.5	0.00061–	4.0	43 944-54 285
V711 Tau	0.0–0.0004	1.0	0.00041–	3.0			42 719-53 703
UZ Lib	0.0–0.0004	1.0	0.00041–	2.5			47 909-54 273
UX Ari	0.0–0.0005	1.0	0.00051–	3.5			44 928-53 440
HU Vir	0.0–0.0001	1.0	0.00011–0.0008	1.0	0.00081–	3.0	47 949-54 065
IL Hya	0.0–0.0005	0.8	0.00051–	3.5			47 129-54 450
XX Tri	0.0–0.0005	1.0	0.00051–	4.0			46 370-54 125
HK Lac	0.0–0.0001	0.7	0.00011–0.00037	1.5	0.00038–	3.2	39 751-54 450
IM Peg	0.0–0.0002	1.0	0.00021–	2.0			43 734-54 450
HD 131156A	0.0–	1.0					39 670-52 414
HD 131156B	0.0–0.0005	1.0	0.00051–	5.0			39 670-52 414
HD 100180	0.0–	1.0					39 898-52 418
HD 201092	0.0–0.00014	1.5	0.00015–0.0005	1.0	0.00051–	2.0	39 670-52 518
HD 201091	0.0–0.0006	1.0	0.00061–	3.0			39 670-52 518
HD 95735	0.0–0.0005	1.0	0.00051–	2.0			39 965-52 419

The values represent the different amplitudes of the cycles (see text).

UZ Lib. The cycle length slowly varies from 4.3 to 3.1-yr. Earlier Oláh et al. (2002) found a cycle length of 4.8-yr. The long-term signal near 15-yr is comparable to the length of the dataset itself, so cannot be established as a cycle.

UX Ari. Its record contains a significant cycle of ∼4.6-yr that decreases to ∼3.6-yr by the end of the record. A long-term signal seems to decrease in parallel with the shorter cycle from ∼25 to ∼15 years; however, that longer period timescale is comparable to the length of the record, so thus not considered significant. On the other hand, that the long cycle changes *in parallel* with the short one strengthens its reliability. We note that Aarum-Ulvås & Henry (2003) report an activity cycle of 25-yr on UX Ari.

HU Vir. The dominant cycle length of this star is ∼5.5–6-yr, in agreement with the values found by Oláh et al. (2000, 2002). The shorter-period signals are considered to be insignificant.

IL Hya. A long gap (of approximately 4 years) occurs in the beginning of the record, which makes the early part of the record unacceptable for our analysis. Hence, we considerably shortened the record for study here; compared to the previous studies of Oláh et al. (2000, 2002, 2007), we cannot study the 13-yr cycle found earlier. However, we confirm the previous result of Oláh et al. (2007) on the changing nature of the short cycle (from 3.5 to 4.3-yr in that paper). The present result shows that a ∼4.4-yr cycle persists throughout the 20-yr record, and a short cycle also appears, increasing from ∼2.7 to ∼3 yr.

XX Tri. Apart from a long trend, only a weak ∼3.8-yr cycle is present with significant amplitude only in the second half of the record.

HK Lac. The first cycle lengths of this star were estimated by Oláh et al. (2000) as ∼6.8 and ∼13-yr. Fröhlich et al. (2006) extended the dataset with measurements from Sonneberg Sky-patrol plates, and not only confirmed the previous results but also found a third cycle with a length of 9.65-yr. The origin of the third cycle lies in the changing cycle lengths of HK Lac, as was first communicated by Oláh (2007). The very beginning of the record was omitted from the present analysis because of scarce sampling. The Sonneberg results start well before the

photometric measurements, thereby lengthening the record to 50 years; the photographic measurements partly overlap the photometry and fill some gaps. The present results, in agreement with all previous ones, shows a cycle varying slowly between ∼5.4 and ∼5.9-yr, together with the cycle increasing from ∼10.0 to ∼13.3-yr.

IM Peg. One cycle of ∼9.0-yr is present, in accordance with the ∼10.1-yr cycle found by Oláh et al. (2002). A long-term signal of 18.9 years is not considered significant, because it is ten years shorter than the record.

5. Results of the time series analysis from Ca II index data

Studying stellar activity cycles was one of the main aims of the Wilson project (e.g. Wilson 1978), and fundamental results on decadal variability have been published from the Ca II index records. Ours is not the first attempt to find not only cycle but also rotational periods from that dataset. However, with the use of our methods we wished to compare the results from photometry of stellar photospheres with those from Ca II H&K spectroscopy, which reflects the variability of chromospheres.

5.1. Rotational periods

The first thorough analysis of rotational modulation from the Ca II index data was carried out by Baliunas et al. (1996a). That work is based on records of 112 stars, among them all six objects of the present investigation. All rotational periods found by Baliunas et al. (1996a) agree with the present results, which is not always the case in later studies of other stars in the sample. Figure 3 shows the period analysis of the six stellar records, all of which were prewhitened with the long-term variability (trends and cycle periods). The results are presented in Table 4 together with periods found in the literature. In all cases typical patterns arising from Fourier analysis of non-stable signals are seen: e.g., differential rotation of the stars produces significant power at
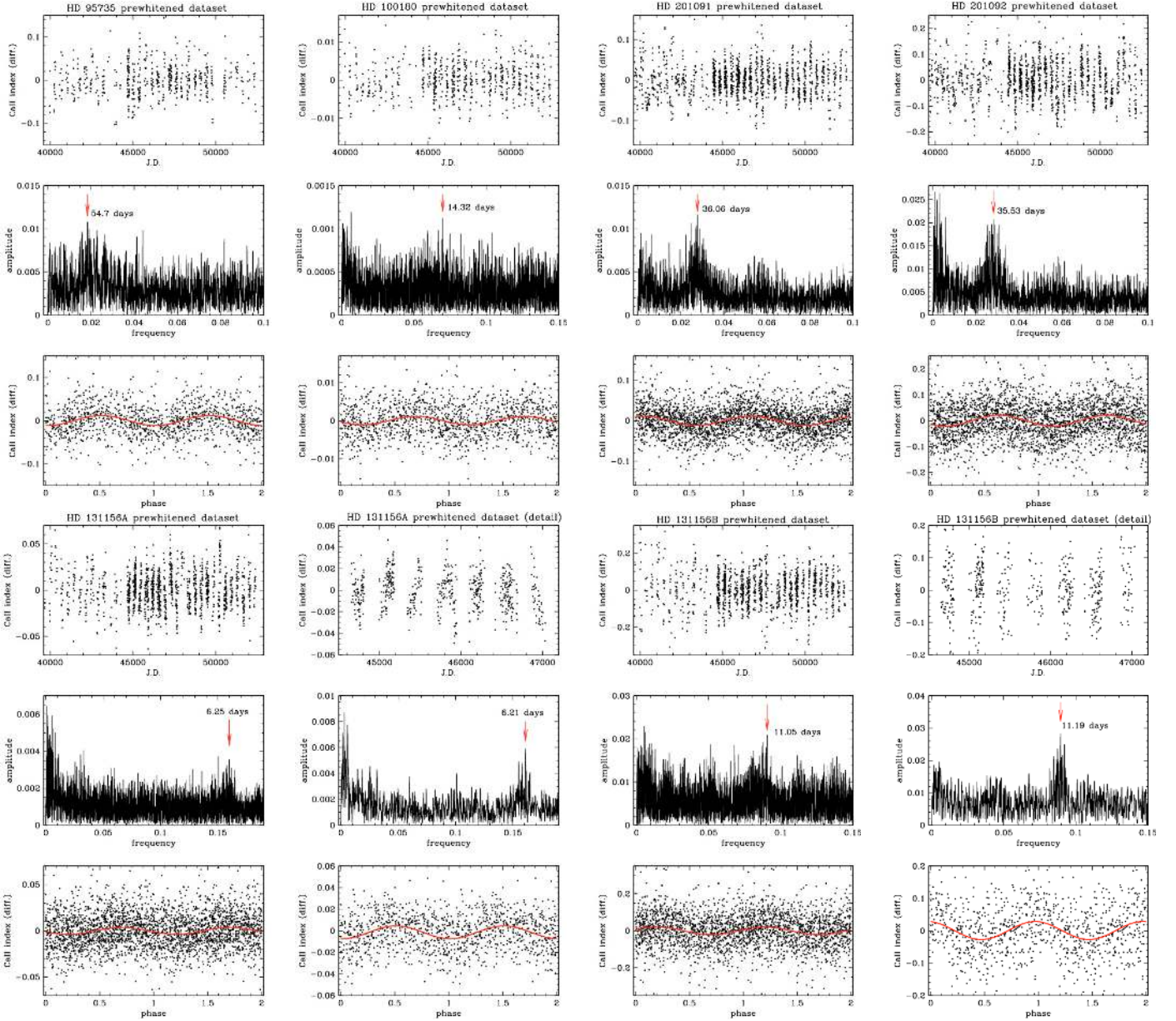
Fig. 3. Rotational periods from Ca II index data. *Upper panel, from left to right*: HD 95735, HD 100180, HD 201091, HD 201092. *Lower panel, from left to right*: HD 1131156A and detail, HD 131156B and detail. Each segment consists of three panels: *top*: data prewhitened with decadal-scale variations; *middle*: power spectra with the rotational period marked; *bottom*: data folded on the derived period.

frequencies around the main rotational frequency of the amplitude spectra.

We split the records into three nearly equal parts in time and repeated the period search. The results are different among the three sets, primarily because of the effects of differential rotation, but short-lived structures appearing and disappearing at different positions may modify the derived periods as well. The values of periods detected in the subsets of the records are given in Table 5. Taking these results into account plus those from the literature, we estimating uncertainties in the mean derived rotational periods of at least a few tenths of a day for shorter periods, and about 1.5–2 days for stars with rotational periods of a few weeks. Seasonal periods determined by Donahue et al. (1996) show a wider range of periods than seen in our analysis because of a multi-seasonal average in our analysis of

several seasons combined as one subset. Baliunas et al. (1996a) and Donahue et al. (1996) used 10 years shorter datasets, and Frick et al. (2004) and Baliunas et al. (2006) the same length records as we use in the current paper. In Fig. 3 (lower panel) we show two examples, HD 131156A and HD 131156B, in which the amplitude spectra of the entire record and part of it yield different periods. In the presence of strong differential rotation but without knowing the rotational profile and the inclination of the star, it is nearly impossible to derive a precise mean rotational period.

5.2. Time-frequency results

Below we present the new results of the cycles of each star individually, and compare them with the previous results.

Table 4. Rotational periods from Ca II index records.

Star	Rotation periods in days				
	(1)	(2)	(3)	(4)	(5)
HD 131156A	6.25	6	6.31	–	8.2
HD 131156B	11.1	11	11.94	–	–
HD 100180	14.3	14	–	38	–
HD 201092	35.5	35	37.84	36	45, 51
HD 201091	36.1	38	35.37	36	44, 47.5
HD 95735	54.7	53	–	–	28.5

(1) Present paper; (2) Baliunas et al. (1996a); (3) Donahue et al. (1996); mean periods; (4) Frick et al. (2004; (5) Baliunas et al. (2006).

Table 5. Rotational periods from Ca II index measurements, for the full datasets and for three subintervals.

Star	all data (days)	1. part (days)	2. part (days)	3. part (days)
HD 131156A	6.25	–	6.21	6.15
HD 131156B	11.1	–	11.2	11.05
HD 100180	14.3	–	14.9	–
HD 201092	35.5	30.2	36.5	35.53
HD 201091	36.1	37.3	36.0	38.4
HD 95735	54.7	–	54.5	–

Values outside 3σ in different subsets indicate differential rotation.

HD 131156A = ξ Boo A. Variability on two time scales are present. The shorter cycle is ~5.5-yr and exhibits a high amplitude in the beginning of the record; the cycle length decreases to ~3.9-yr at the record's end. A longer period variability is also apparent, with a characteristic timescale of ~11 yr in the middle of the record. Baliunas et al. (1995) marked the decadal variability of the record as "*var*", which means *"significant variability without pronounced periodicity, on timescales longer, than 1-yr but much shorter than 25-yr..."*, and this is in accordance with our results for the record that is ten years longer; also, Baliunas et al. (2006) find a long cycle of 13.2 years.

HD 131156B = ξ Boo B. Only one long-term periodicity is found, and only in the beginning of the record, approximately ~4.3-yr, although a secular change is also evident. Baliunas et al. (1995) remark as *long*, i.e., signifcant variability is found, which is longer than 25 years.

HD 100180 = 88 Leo. We derive a more or less constant cycle of ~3.5-yr, which persists nearly through the entire record, but its amplitude is strong in the first half of the record and decreases thereafter. Another variable cycle of ~13.7-yr appears in the beginning of the record; the period decreases to ~8.6-yr by the end of the record, in agreement with the earlier results of Oláh et al. (2007). Our results in the beginning of the dataset are similar to those found by Baliunas et al. (1995), who found two cycles, ~3.56 and ~12.9-yr in the record shorter by ten years. Analysing the full record, Frick et al. (2004) found periodicities of ~3.7 and ~10.1-yr. The short cycle is consistent with our result, the ~10.1-yr value may be an averaged mean value of the long variable cycle we detect.

HD 201092 = 61 Cyg B. The record for this star also exhibits two activity cycles: one is ~4.7-yr and persists thoughout the record, the other has a timescale of ~10–13 years. Both periodicities have variable amplitudes. The long cycle was estimated in previous studies as 11.4, 11.1, and 11.7-yr by Baliunas et al. (1995), Frick et al. (2004) and Baliunas et al. (2006), respectively.

Table 6. Derived activity cycles.

Star	Rotation period[a] (days)	Cycle lengths (years)
AB Dor	0.515	3.3, L
LQ Hya	1.601	2.5, 3.6, 7.0→12.4
V833 Tau	1.788	2.2, 5.2, 27-30, L
V410 Tau	1.872	4.1←5.2, 6.5→6.8
EI Eri	1.947	2.9↔3.1, 4.1↔4.9, 14.0
FK Com	2.400	4.5↔6.1, L
V711 Tau	2.838	3.3, 5.4, 8.8←17.9
UZ Lib	4.768	3.1←4.3, L
UX Ari	6.437	3.6←4.6, L
HU Vir	10.388	5.7, L
IL Hya	12.905	2.7→3.0, 4.4, L
XX Tri	23.969	3.8, L
HK Lac	24.428	5.4→5.9, 10.0→13.3, L
IM Peg	24.649	9.0, L
HD 131156A	6.25	3.9←5.5, 11.0
HD 131156B	11.1	4.3, L
HD 100180	14.3	3.5, 8.6←13.7
HD 201092	35.5	4.7, 11.5
HD 201091	36.1	3.6, 6.2↔7.2
HD 95735	54.7	3.4↔3.9, 11.0

The cycle lengths, given in years, are listed in order of increasing value. For changing cycle periods, arrows show the direction of the change between the extreme values, "L" denotes multi-decadal variations.
[a] The orbital period is given in the case of a synchronised binary.

HD 201091 = 61 Cyg A. The high amplitude cycle seen in the record of this star has a mean length of 6.7-yr, which slowly changes between 6.2 and 7.2-yr. A shorter, significant cycle is found in the first half of the record with a characteristic timescale of ~3.6-yr. Probably because of the changing and double nature of the main cycles, previous determinations are slighly different but still consistent with our result. Baliunas et al. (1995) derived 7.3-yr, Frick et al. (2004) found 7.12-yr and finally Baliunas et al. (2006) estimated 5.43-yr. However, the most interesting comparison to our results for HD 201091 is that of Frick et al. (1997, their Fig. 5, bottom left panel, and Fig. 6, lower panel). They derived a changing cycle between ~6.7 and 7.9-yr, while the record at that time was about ten years shorter than now. Comparing Fig. 5 of Frick et al. (1997) to Fig. 4, (bottom, middle), it is seen that the results are similar, though, because of our higher frequency resolution we could resolve two cycles in the beginning of the record.

HD 95735 = GJ 411. The stronger cycle of this star is ~3.9-yr, which is slightly shorter (3.4-yr) in the beginning of the record. A longer, 11-yr cycle is also present with a smaller amplitude. Baliunas et al. (1995) classify the record as *var* (see the explanation at HD 131156A). The long cycle was estimated as ~11.3-yr by Baliunas et al. (2006). The rotational period found by Baliunas et al. (2006) is 28.5-d and by us 54.7-d; the shorter result possibly arises from the non-sinusoidal nature of the rotational modulation caused by two distinct activity centres at spatially separated stellar longitudes.

6. Discussion

6.1. Cycle lengths

The results of our analysis are summarised in Table 6, where the cycle lengths are listed in order of increasing value. In cases of changing cycle periods, arrows show the direction of the change between the extreme values (increasing, decreasing, or both). An
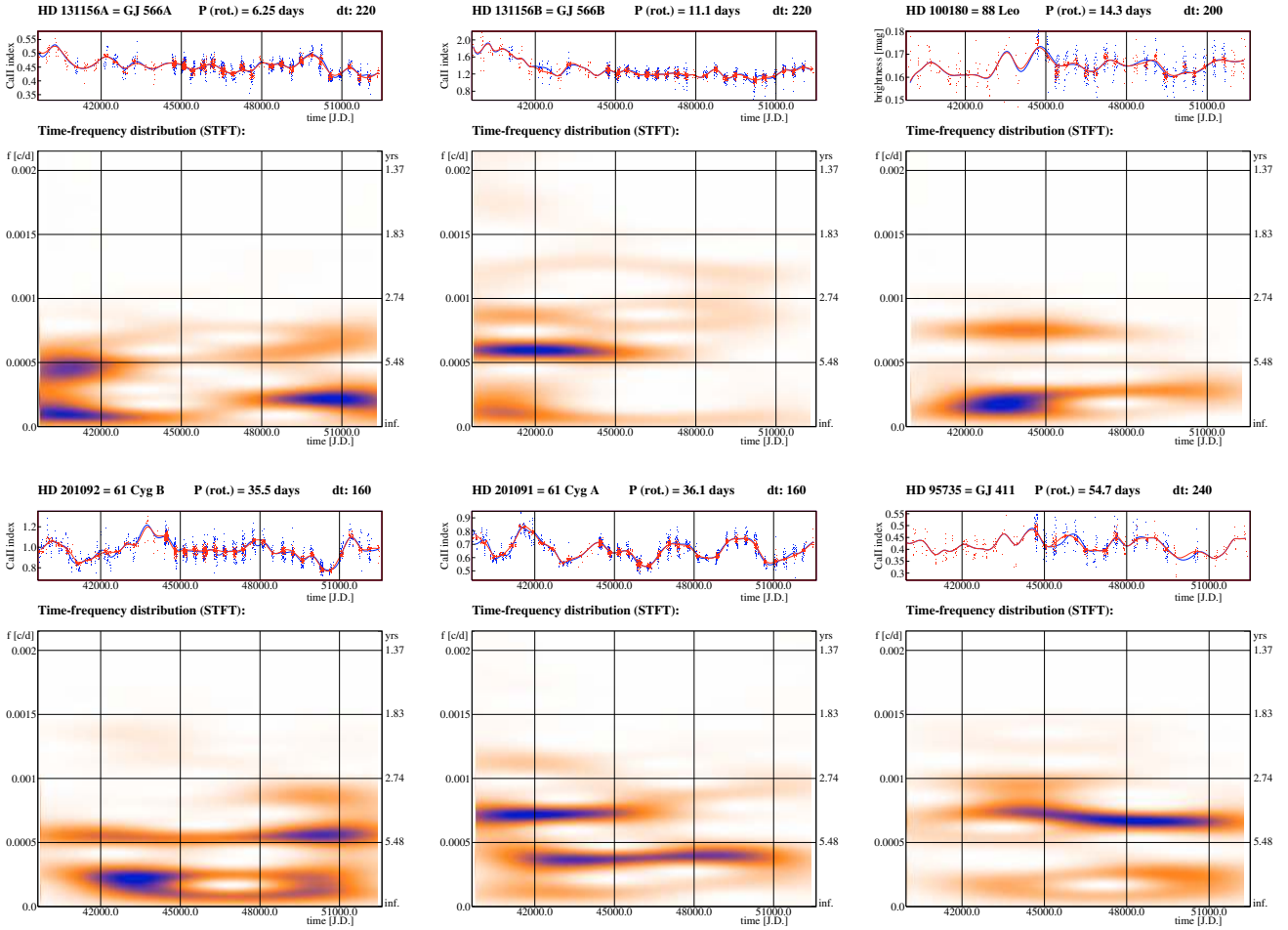
Fig. 4. The STFT of the Ca II sample, panels, and colour codes as in Fig. 2. *Top*: HD 131156A, HD 131156B, HD 100180, *bottom*: HD 201092, HD 201091, HD 95735. Details are in the text.

"L" denotes a multi-decadal variation, which may occur in addition to the detected cycle(s); however, a timescale cannot be given because of the insufficient length of the record to resolve the longer period.

Most of the stars show multiple cycles. Those stars for which we list only one cycle usually show variability on longer timescales. The lengths of the records are too short to verify additional, longer cycles for AB Dor, HU Vir, XX Tri, IM Peg, and HD 131156B (see Table 6).

The cycle lengths are not strictly constant or randomly variable, but show *systematic* changes during the period of observations. We see two kinds of systematically changing cycles. The first is characterised by a cycle length that oscillates between a lower and an upper value, and the second by a cycle length exhibiting a secular variation, i.e., an increase or a decrease. However, these continuously increasing or decreasing cycle lengths may reverse over a longer observational period than currently available.

In Paper I we studied the multi-decadal variability of the solar Schwabe and Gleissberg cycles during the past 250 years from Sunspot Number records. In Fig. 2 (bottom panel) of Paper I we used the same method (STFT) as for the stars in the present paper. The results look similar; i.e., for the Sun, one cycle (Schwabe) varies between limits, while the longer one (Gleissberg) continually increases. However, the results for a longer time displayed in Fig. 8 in Paper I indicated that the Gleissberg cycle of the Sun also varies between limits on a scale

of ~50–140-yr, but to confirm the variability of the Gleissberg cycle required a longer, 500-yr record. By analogy from the analysis of the longer solar record, a long-term trend may suggest an increasing or decreasing multidecadal cycle that is presently unresolved in the stellar records of short duration.

Another feature of interest in our analysis of cycle lengths in stellar records is that of the dominant (highest amplitude) cycle rapidly switching to another one. In EI Eri in the beginning of the dataset the long, ~14-yr cycle is dominant, and the short cycle of about 4.5-yr is only weakly present. Around JD 2 447 000 the amplitude of this short cycle increases considerably, and that high amplitude cycle persists for more than 12-yr (~3 short cycles). Later the longer cycle again dominates. (The beginning is uncertain because of sparse data, but the end of the record is well sampled.) A similar pattern is seen in LQ Hya.

Interesting feature is found in V410 Tau, EI Eri, and UX Ari: two cycles in each of them that are not harmonics of each other, are changing parallel. This finding points towards the common physical origin of these cycles, i.e., that both cycles are produced by the same dynamo.

6.2. Relations

The cycle lengths of two stars were excluded from further analysis. The first is the shortest period, ultrafast rotating ($P_{rot} = 0.459$ d), M1-2 dwarf star EY Dra, which might show a cycle of around 1 year from observations made every two months with
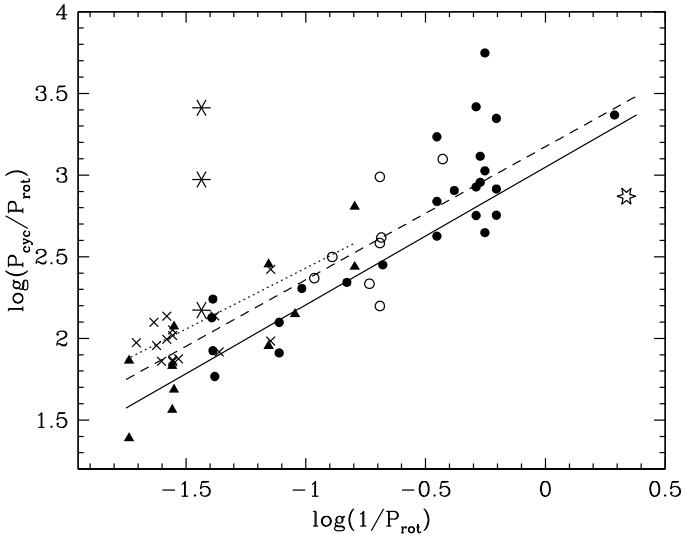
Fig. 5. The quantity $\log(P_{cyc}/P_{rot})$ vs. $\log(1/P_{rot})$, as in Baliunas et al. (1996b). The plot includes the results of the present investigation and those from the literature: Messina & Guinan (2002, circles) and Frick et al. (2004, crosses). The results from the current photometric investigation are marked by filled dots, and filled triangles denote the results from the Ca II records (HD 95735 is excluded from the fits). For changing cycles mean values are plotted. The different cycles of the Sun are represented by stars. A hexagon in the far right shows the position of the fast rotator EY Dra (excluded from the fits). The dotted line shows the original relation from Baliunas et al. (1996b), dashed line is the fit to all results, including those from the literature, and the solid line is the relation for the shortest cycle lengths determined by us.
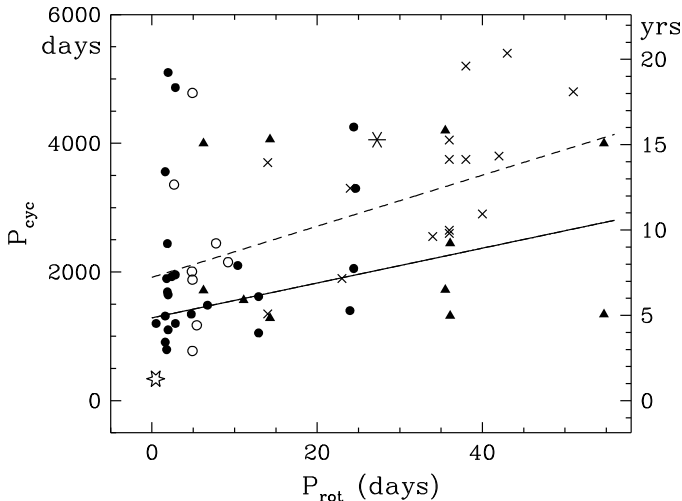
Fig. 6. The rotational period-cycle period diagram, with symbols as in Fig. 5. The dashed line is the fit to all results including the ones from the literature, and the solid line is the relation for the shortest cycle lengths determined by us.

gaps of only 4 months (see Vida 2007), but that cycle is uncertain. The other is the star with the longest rotation period in our sample, HD 95735 (P_{rot} = 54.7 d), a dwarf of spectral type M2, which is rotating ~120 times slower than EY Dra, but has the same spectral type. Those two stars are the only M dwarfs that have reported activity cycles and have the shortest (EY Dra) and longest (HD 95735) rotation periods, which are plotted in Figs. 5 and 6, but are excluded from the fits. Their internal structure may differ significantly from the other stars in the sample.

Graphic representation of the results are given in Fig. 5 on a log–log scale of P_{cyc}/P_{rot} vs. $1/P_{rot}$, as in the paper of Baliunas et al. (1996b, Fig. 1). The cycle period is expected to scale $\sim D^{\iota}$ where ι is the slope of the relation and D is the dynamo number. The slope for the results in Baliunas et al. (1996b) was 0.74 (dotted line in Fig. 5), and we get 0.81 ± 0.05 for all the results from the present paper and from Messina & Guinan (2002), and Frick et al. (2004). The fit to the shortest cycles determined by us gives a slope of 0.84 ± 0.06.

The log–log representation of the cycle period normalised by the rotation period gives a direct relation to the dynamo number. In comparison, the direct representation of the cycle vs. rotational periods in Fig. 6 has information about the tightness of the relation that is suppressed a little in Fig. 5 by the normalisation and the scale. All symbols of Fig. 6 are the same as in Fig. 5. The Gleissberg timescale of the Sun is not plotted, because even its shortest value (50-yr, i.e., about 18 000-d) would compress the figure along the y-axis. The slope of the relation for all the results of the present paper together with the values from the literature is 39.7 ± 10.6, whereas is 27.1 ± 12.1 for the newly determined shortest cycles; i.e., the relation is significant for all the data considered together, and marginal when only the shortest cycles are considered.

However, an important warning should be recalled from Paper I: cycle periods of 1–2-yr recovered from records with approximately yearly gaps are highly uncertain if not insignificant. Hence, the lower end of the diagrams in Figs. 5 and 6, i.e., at the shorter rotational periods, the shortest cycles simply cannot be recovered with certainty, thereby distorting the fitted relations.

Finally, we note (i) that the stars studied in this paper and those from the literature that are plotted together in Figs. 5 and 6 represent a wide range of objects in the context of spectral types, characteristics of the observational data (photometry, spectroscopy, lengths of the records); and (ii) that the sample consists of both single stars and stars in binary systems. Therefore, while we find a general trend between the rotational periods and cycle timescales, a much tighter correlation cannot be expected.

7. Summary

We analysed continuous photometric and spectroscopic records on multi-decadal periods of 20 active, cool stars using short-term Fourier transform and studied the patterns of their activity cycles. We found that

– 15 stars show definite, multiple cycles, the others probably do,
– most of the cycle lengths are found to change systematically,
– in three cases two cycles are changing parallel,
– and the relation between the rotational periods and cycle lengths is confirmed for the inhomogeneous set of active stars consisting of dwarfs and giants and of single and binary systems.

Moss et al. (2008) depict a complicated picture of symmetry properties derived from models of stellar magnetic fields, while expecting that properties of observed stellar cycles may offer progress on the problem. The present paper gives twenty different examples (21 together with the Sun from Paper I) of multiple cycles that can arise from *"dynamos operating in significantly supercritical regimes"*. The observed modulations in amplitude and cycle lengths may stem from cyclic quadrupolar components superimposed on a dipole cycle, as suggested by

Moss et al. (2008). The *predictability* of the cycle patterns at the moment is very limited. We are able to describe from observations with mathematical tools what happened in the past, but for the future only trends and tendencies can be suggested. Further detailed theory is needed to model the complicated cycle structures we observe in stars and in the Sun. Thorough modelling the observed cycle patterns may be the only way for the present to predict with success the future patterns of the Sun and the stars.

References

Aarum-Ulvas, V, & Henry, G. W. 2003, A&A 402, 1033
Baliunas, S. L., Donahue, R. A., Soon, W., et al. 1995, ApJ, 438, 269
Baliunas, S. L., Sokoloff, D., & Soon, W. 1996a, ApJ, 457, L99
Baliunas, S. L., Nesme-Ribes, E., Sokoloff, D., & Soon, W. 1996b, ApJ, 460, 848
Baliunas, S. L., Frick, P., Moss, D., et al. 2006, MNRAS, 365, 181
Berdyugina, S. V., & Henry, G. 2007, ApJ, 659, L157
Berdyugina, S. V., Pelt, J., & Tuominen, I. 2002, A&A, 394, 505
Bushby, P. J., & Tobias, S. M. 2007, ApJ, 661, 1289
Cameron, R., & Schüssler, M. 2007, ApJ, accepted
Detre, L. 1971, Inf. Bull. Var. Stars, No. 520 (Editor's note)
Donahue, R. A., Saar, S. H., & Baliunas, S. L. 1996, ApJ, 466, 384
Durney, B. R., & Stenflo, J. O. 1972, Ap&SS, 15, 307
Frick, P., Baliunas, S. L., Galyagin, D., Sokoloff, D, & Soon, W. 1997, ApJ, 483, 426
Frick, P., Soon, W., Popova, E., & Baliunas, S. 2004, New Astron., 9, 599
Fröhlich, H.-E., Kroll, P., & Strassmeier, K. G. 2006, A&A, 454, 295
Geyer, E. 1978, Astronomische Gesellschaft, Mitteilungen, 43, 187
Hartmann, L., Dussault, M., Noah, P. V., Klimke, A., & Bopp, B. W. 1981, ApJ, 249, 662
Henry, G. W., Eaton, J. A., Hamer, J., & Hall, D. S. 1995, ApJ, 97, 513

Innis, J., Budding, E., Oláh, K., et al. 2008, IBVS, No. 5832
Järvinen, S. P., Berdyugina, S. V., Tuominen, I., Cutispoto, G., & Bos, M. 2005, A&A, 432, 657
Kjurkchieva, D. P., & Marchev, D. V. 2005, A&A, 434, 221
Kolláth, Z., & Oláh, K. 2009, A&A, 501, 695 (Paper I)
Kővári, Zs., Strassmeier, K. G., Granzer, T., et al. 2004, A&A, 417, 1047
Kron, G. E. 1947, PASP, 59, 261
Lanza, A. F., Piluso, N., Rodono, M., Messina, S., & Cutispoto, G. 2006, A&A, 455, 595
Lockwood, G. W., Skiff, B. A., Henry, G. W., et al. 2007, ApJS, 171, 260
Messina, S., & Guinan, E. F. 2002, A&A, 393, 255
Messina, S., & Guinan, E. F. 2003, A&A, 409, 1017
Moss, D., Saar, S. S., & Sokoloff, D. 2008, MNRAS, 388, 416
Oláh, K. 2007, in Highlights of Astronomy, IAU XXVL GA, 14–25 August 2006, Prague, ed. Karel A. van der Hucht, 14, 283
Oláh, K., & Strassmeier, K. G. 2002, in Proc. 1st Potsdam Thinkshop on Sunspots and Starspots, ed. K. G. Strassmeier, AN 323, 3/4, 361
Oláh, K., Kővári, Zs., Bartus, J., et al. 1997, A&A, 321, 811
Oláh, K., Kolláth, Z., & Strassmeier, K. G. 2000, A&A, 356, 643
Oláh, K., Strassmeier, K. G., Kővári, Zs., & Guinan, E. F. 2001, A&A, 372, 119
Oláh, K., Strassmeier, K. G., & Granzer, T. 2002, AN, 323, 5, 453
Oláh, K., Korhonen, H., Kővári, Zs., Forgács-Dajka, E., & Strassmeier, K. G. 2006, A&A, 452, 303
Oláh, K., Strassmeier, K. G., Granzer, T., Soon, W., & Baliunas, S. L. 2007, AN, 328, 1072
Radick, R. R., Lockwood, G. W., Skiff, B. A., & Baliunas, S. L. 1998, ApJS, 118, 239
Ribárik, G., Oláh, K., & Strassmeier, K. G. 2003, AN, 324, 202
Saar, S. H., & Brandenburg, A. 1999, ApJ, 524, 295
Schwabe, H. 1843, AN, 20, 284
Stelzer, B, Fernández, M, Costa, V. M. et al. 2003, A&A, 411, 517
Strassmeier, K. G. 2002, AN, 323, (3/4), 309
Strassmeier, K. G., Boyd, L. J., Epand, D. H., & Granzer, Th. 1997a, PASP, 109, 697
Strassmeier, K. G., Bartus, J., Cutispoto, G., & Rodono, M. 1997b, A&AS, 125, 11
Valenti, J. A., & Fischer, D. A. 2005, ApJS, 159, 141
Vaughan, A. H., Preston, G. W., & Wilson, O. C. 1978, PASP, 90, 267
Vida, K. 2007, AN, 328, 817
Vogt, S. S., Hatzes. A. P., & Misch, A. 1999, ApJS, 121, 547
Washuettl, A., Kővári, Zs., Foing, B. H., et al. 2008, A&A, submitted
Wilson, O. C. 1968, ApJ, 153, 221
Wilson, O. C. 1978, ApJ, 226, 379